Tribology Transactions

ISSN: 1040-2004 (Print) 1547-397X (Online) Journal homepage: https://www.tandfonline.com/loi/utrb20

Wear Behavior of Magnesium Alloy AZ91 Hybrid Composite Materials

B. M. Girish, B. M. Satish, Sadanand Sarapure, D. R. Somashekar & Basawaraj

To cite this article: B. M. Girish, B. M. Satish, Sadanand Sarapure, D. R. Somashekar & Basawaraj (2015) Wear Behavior of Magnesium Alloy AZ91 Hybrid Composite Materials, Tribology Transactions, 58:3, 481-489, DOI: 10.1080/10402004.2014.987858

To link to this article: https://doi.org/10.1080/10402004.2014.987858

Accepted author version posted online: 16 Dec 2014.
Published online: 23 Feb 2015.

Tribology Transactions, 58: 481–489, 2015

ISSN: 1040-2004 print / 1547-397X online
DOI: 10.1080/10402004.2014.987858

stle
Society of Tribologists and Lubrication Engineers

Wear Behavior of Magnesium Alloy AZ91 Hybrid Composite Materials

B. M. GIRISH[1], B. M. SATISH[1], SADANAND SARAPURE[2], D. R. SOMASHEKAR[3], and BASAWARAJ[1]
[1]Department of Mechanical Engineering, East Point College of Engineering and Technology, Bangalore 560 049, Karnataka, India
[2]Department of Mechanical Engineering, Acharya Institute of Technology, Bangalore 560 107, Karnataka, India
[3]Department of Mechanical Engineering, Raj Kumar Goel Institute of Technology, Ghaziabad, 201 003 Uttar Pradesh, India

The influence of hybrid reinforcements including silicon carbide and graphite particles with a size 37–50 μm on the wear characteristics of AZ91 magnesium alloy was studied. The dry sliding wear test was conducted using a pin-on-disc wear testing machine in the load range of 20 to 80 N at different sliding velocities in the range of 1.047 to 2.618 m/s. The results show that the wear resistance of composites was much better than that of the base matrix material under the test conditions. At a speed of 1.047 m/s and load of 40 N, the wear rate (mm^3/km) of the unreinforced alloy was 6.3, which reduced to 3.8 in the case of 3% reinforced composite. The antiwear ability of magnesium alloy composite was found to improve substantially with the increase in silicon carbide and graphite content from 1 to 3% by weight and the wear rate was found to decrease considerably. At a speed of 1.047 m/s and load of 80 N, the wear rate (mm^3/km) reduced from 11.8 to 9.1 when the reinforcement content increased from 1 to 3%. However in both the unreinforced alloy and reinforced composite, the wear rate increased with the increase in load and sliding velocity. An increase in the applied load increases the wear severity by changing the wear mechanism from abrasion to particle cracking-induced delamination. The worn surface morphologies of the composite containing 3% reinforcement by weight for the sliding velocity of 1.047 m/s were examined using scanning electron microscopy. Different wear mechanisms, namely, abrasion, oxidation, and delamination, have been observed.

KEY WORDS

Unlubricated Wear; Graphite; SiC; Magnesium Alloys

INTRODUCTION

Magnesium alloy products are being used increasingly in automobile and aerospace industries due to their low density, high specific strength, high specific stiffness, good damping characteristics, and excellent machinability and castability (Aydin and Findik *(1)*; Qi, et al. *(2)*; Zheng, et al. *(3)*). At present, the most commonly used magnesium alloy is AZ91 alloy.

Wear is a serious problem in many engineering applications, such as bearings, moving parts, engine parts, etc. Although it is only a surface phenomenon, it can completely undermine the mechanical function of engineering parts. It can cause structural failure directly, reduce the fine tolerances, and destroy the surface finish. In the last two decades, many studies have been done on metal matrix composites (MMCs) involving aluminum, magnesium, and zinc alloys as base metals (Zhai, et al. *(4)*; H. J. Zhang, et al. *(5)*; L. Zhang, et al. *(6)*). Particles, fibers, and rare earth elements are used as reinforcements to improve the wear properties of magnesium alloy (Rao, et al. *(7)*; Tu and Yang *(8)*). Most studies have focused on SiC and TiC particle-reinforced magnesium-based MMCs. However, investigations on self-lubricating composites with graphite as the addition are rather limited (Lu, et al. *(9)*; Gu, et al. *(10)*). Qi, et al. *(11)* investigated the formation of a graphite film during the sliding process of magnesium-based MMCs.

Studies on hybrid composites have been reported (Baradeswaran and Elaya Perumal *(12)*; Ram Prabhu, et al. *(13)*; Zhan and Zhang *(14)*) where two ceramic materials are used to reinforce an alloy. Baradeswaran and Elaya Perumal *(12)* have studied the wear behavior of Al_2O_3 and graphite-reinforced aluminum alloys and found that the resulting composite exhibited superior wear resistance. Ram Prabhu, et al. *(13)* studied the tribological behavior of SiC and graphite-reinforced hybrid composites for brake applications and reported superior wear properties. Further, it is has been reported that usage of a solid lubricant like graphite stabilizes friction at high temperatures (Zhan and Zhang *(14)*) and the presence of graphite in hybrid composites improves thermal conductivity, machinability, damping, and antiseizure properties.

A literature survey (Baradeswaran and Elaya Perumal *(12)*; Ram Prabhu, et al. *(13)*; Zhan and Zhang *(14)*) suggests that most of the work on hybrid composites is in the area of aluminum alloys. This work is of particular significance in view of the limited research that has been done in the field of magnesium alloy–based hybrid composites. The purpose of the present study is to investigate the feasibility of fabrication of AZ91 magnesium alloy hybrid MMCs reinforced with two reinforcement materials,

Manuscript received August 22, 2014
Manuscript accepted November 10, 2014
Review led by David Burris
Color versions of one or more of the figures in the article can be found online at www.tandfonline.com/utrb.

namely, silicon carbide and graphite particulates, and to understand their effect on the wear behavior of the composites. Graphite was used in the present study because it is a widely used solid lubricant, the addition of which, however, lowers the hardness and strength of the resulting composite. Hence, SiC has been added in order to compensate for such losses. In the present study, the wear resistance of the composites is discussed, in particular, the effect of the reinforcement addition on the dry sliding wear behavior. Changes in the wear mechanisms under different conditions along with the morphology of the wear surface were also studied.

EXPERIMENTAL PROCEDURE

AZ91 magnesium alloy, whose chemical composition is given in Table 1, was used as the base matrix alloy. Melting was carried out at 680°C in a mild steel crucible and during the melting process, the oxidation of the surface of the melt was protected using Magrex60, supplied by Foseco (India). Magrex60 is an agent that acts like a flux and prevents oxidation of magnesium, without which handling of magnesium at higher temperatures is not possible. Usage of such flux in magnesium casting operations has been reported elsewhere (Sahin and Acilar *(15)*). The reinforcement percentage of silicon carbide and graphite particles was varied from 1 to 3% in 1 wt% increments. The vortex method was used to prepare the composite specimens. During this process, the uncoated and preheated reinforcements were introduced after defluxing into the vortex created in the molten alloy under an inert atmosphere. An aluminite-coated mechanical impeller was used to create the vortex. The melt was thoroughly stirred, degassed, and poured into spilt-type preheated metal molds.

Samples for microscopic examination were prepared as per ASTM standard E3 and etched with Nital agent and examined under an optical microscope (ECLIPS 150, Nikon, Japan). The wear specimens were tested under unlubricated conditions as per ASTM standard G99 using a pin-on-disc sliding wear testing machine (Ducom TR-20 Wear and Friction Monitor) consisting of an EN24 steel disc (BHN 229) with a diameter of 200 mm as the counterface on which the test specimen was slid. Three specimens were tested for each test condition and the standard deviation did not exceed 5%.

A volume loss method was adopted in the present study in which pins of 6 mm diameter and 15 mm length were used for the test. The disc was cleaned before and after every test with acetone to remove any possible traces of grease and other surface contaminants. The duration of the tests was 60 min. Loads of 20 to 80 N in steps of 20 N were used. The speeds of the disc employed were 200 to 500 rpm in steps of 100 rpm at an average distance of 100 mm from the center of the disc, resulting in velocities of 1.047, 1.57, 2.09, and 2.618 m/s, respectively.

TABLE 1—CHEMICAL COMPOSITION OF AZ91 ALLOY (%)

Al	Zn	Si	Mn	Fe	Cu	Ni	Mg
9.0	1.0	0.035	0.035	0.005	0.0005	0.001	Balance

The wear rate was calculated using the following relation and has been used by Sharma, et al. *(16)* and Mondal and Kumar *(17)*:

$$\text{Wear rate} = \frac{\text{Volume of material removed (mm}^3\text{)}}{\text{Sliding distance (km)}}.$$

Sliding distance (km) = $2\pi r \times \text{Rpm} \times$ time in minutes, where r = the distance of wear track from the center of the disc.

The worn surface was cleaned to remove the loose wear debris and then observed using scanning electron microscopy (SEM) equipped with energy-dispersive X-ray spectrometry (EDS) to verify the dominant wear mechanism.

RESULTS AND DISCUSSION

Microstructure

Figure 1a shows the optical microstructure of magnesium alloy without any reinforcement, and Figs. 1b, 1c, and 1d show the microstructure of the hybrid composite reinforced with 1% SiC and 1% graphite, 2% SiC and 2% graphite, and 3% SiC and 3% graphite particles, respectively. The optical microscopy investigations show a uniform distribution of reinforcement in the matrix. Silicon carbide and graphite particle reinforcements remained well bonded to the matrix and no defects were found.

Effect of Load and Sliding Velocity on the Wear Rate

The wear behavior of composites containing different contents of silicon carbide and graphite particles was determined and compared to that observed in the base alloy. The results were averaged to obtain the final wear rate from three pin specimens at each specified load and sliding velocities of 1.047, 1.57, 2.09, and 2.618 m/s, which are presented graphically in Figs. 2 to 5. The wear rate of unreinforced alloy is also plotted along with the composites for comparison. It is found from the graph that the wear rate of the both unreinforced alloy and composites increase with an increase in load. However, the wear rate of the composite specimens is significantly lower than that of the base

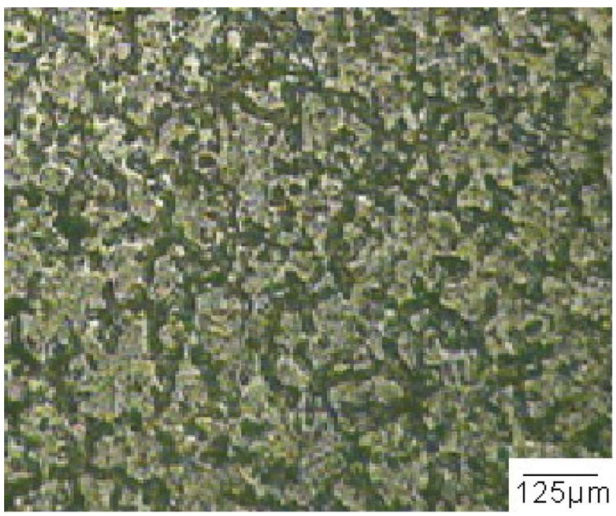

Fig. 1a—Optical microstructure of AZ91 alloy with 0% reinforcement.

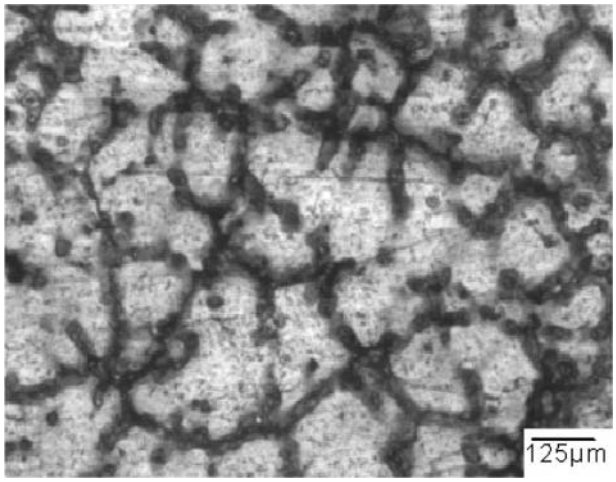

Fig. 1b—Optical microstructure of AZ91 with 1 wt% SiC- and 1 wt% graphite-reinforced composite.

alloy. It is evident from the graphs shown in Figs. 2 to 5 that the wear rate of each composite specimen was reduced with an increase in reinforcement.

It is evident from the graphs that there exists a certain applied load—that is, a transition phenomenon—at which there is a sudden increase in the wear rate of both reinforced as well as unreinforced materials. However, the transition loads for the composites were much higher than that observed for the base alloy. In addition, the transition load increased with an increase in reinforcement content.

It was observed from the graph in Fig. 2 that the unreinforced matrix alloy showed a transition from mild to severe wear at a load of 40 N when tested at a sliding velocity of 1.047 m/s. The same is observed at 20 N when tested at a sliding velocity of 1.57 m/s. Similarly, the composite with 1 to 3% reinforcement shows a transition at 60 N when tested at a sliding velocity of 1.047 m/s. It was found that in the composites of 1 to 2% reinforcement, the transition occurs at a load of 40 N when tested at sliding velocities of 1.57 and 2.09 m/s. However, for the composite with 3% reinforcement, the transition load is still higher at 60 N when tested at sliding velocity of 1.57 and 2.09 m/s. At

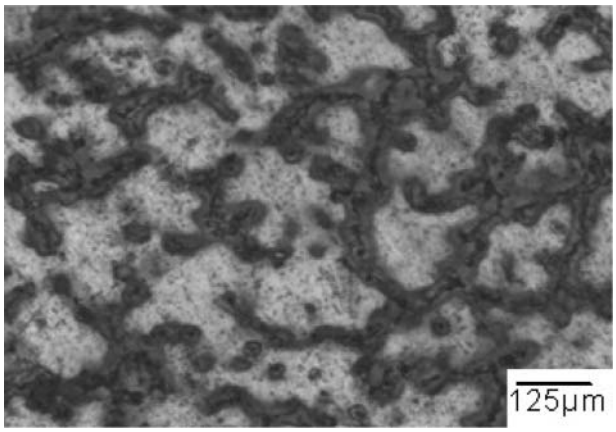

Fig. 1c—Optical microstructure of AZ91 with 2 wt% SiC- and 2 wt% graphite-reinforced composite.

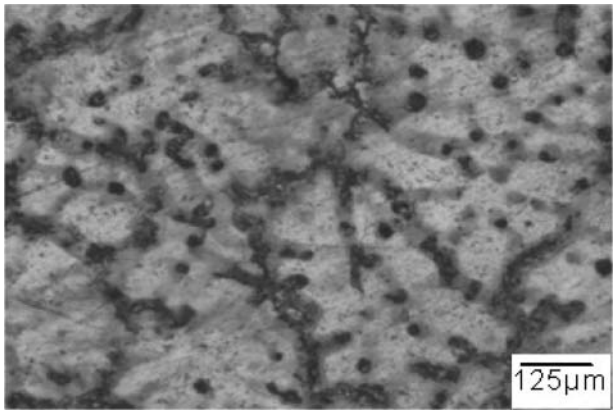

Fig. 1d—Optical microstructure of AZ91 with 3 wt% SiC- and 3 wt% graphite-reinforced composite.

higher sliding velocities, the alloy and composites show mild to severe wear at a lower load only. However, the wear rate for composites is lower even at high speeds when compared to the alloy at low load. It is evident from Figs. 2 to 5 that the presence of reinforcement delays the transition from mild to severe wear.

It follows from the results obtained that a comparatively lower wear rates exist at lower loads, thereby indicating the regime of mild wear, in which the composite shows significantly better wear resistance than the alloy counterpart. At higher loads severe wear occurs, leading to seizure of the materials.

The above observations clearly indicate that the sliding velocity employed has a significant effect on the wear rate transition

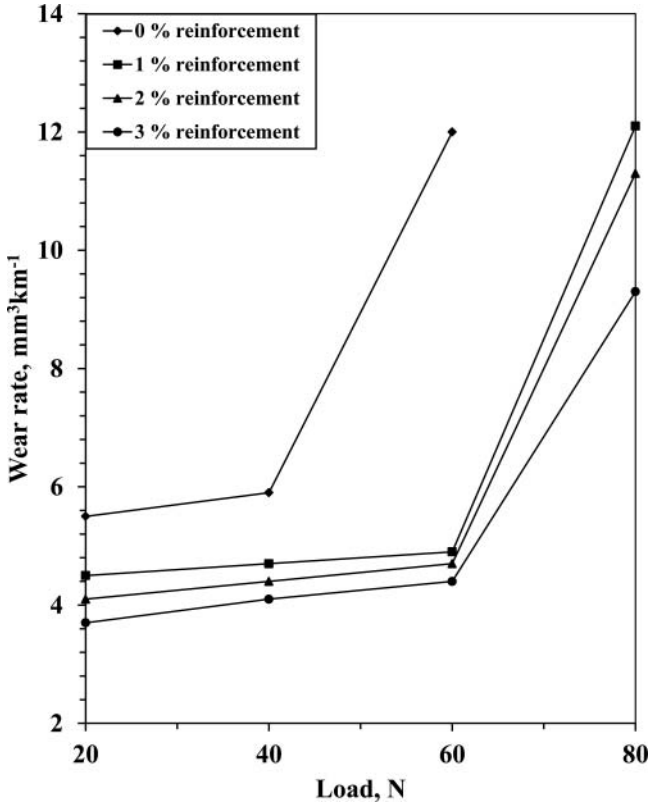

Fig. 2—Graph of wear rate vs. load at a speed of 1.047 m/s and test duration of 60 min.

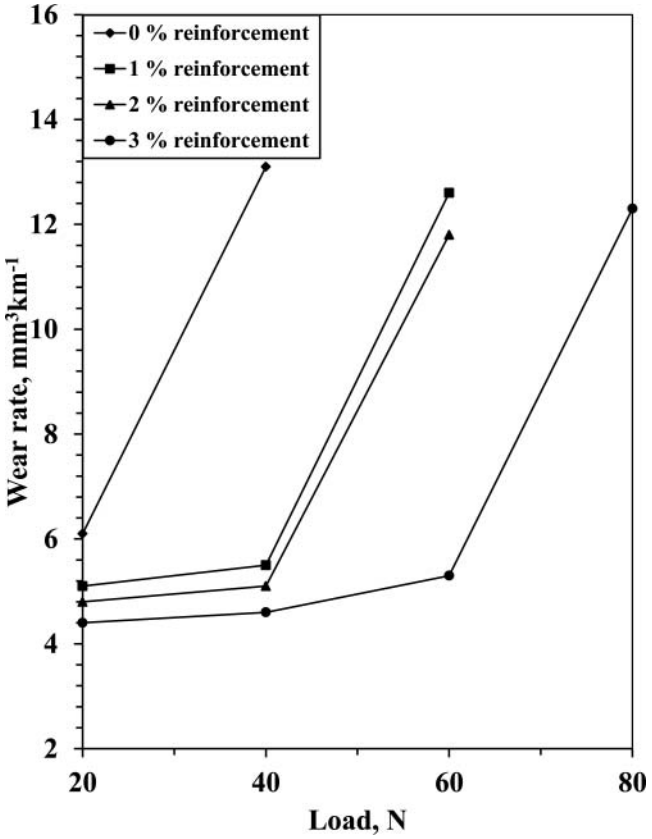

Fig. 3—Graph of wear rate vs. load at a speed of 1.57 m/s and test duration of 60 min.

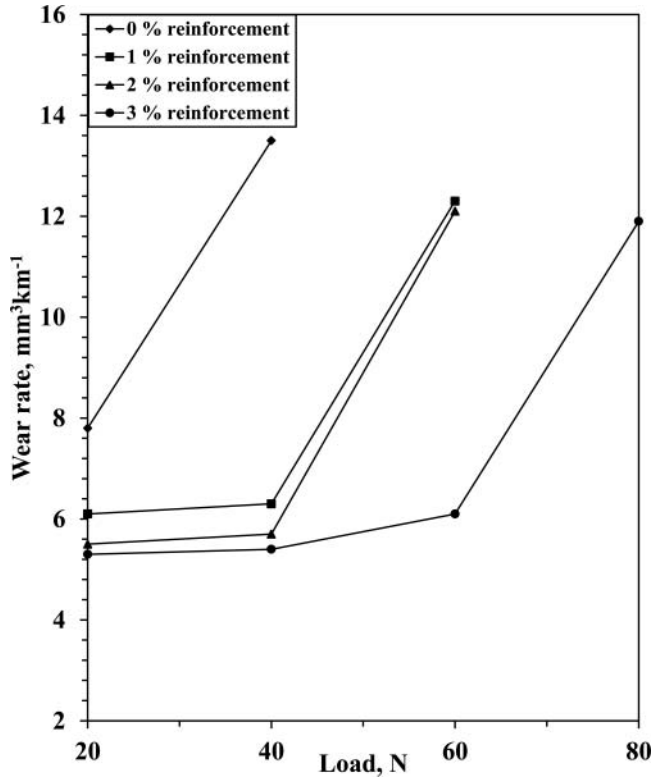

Fig. 4—Graph of wear rate vs. load at a speed of 2.09 m/s and test duration of 60 min.

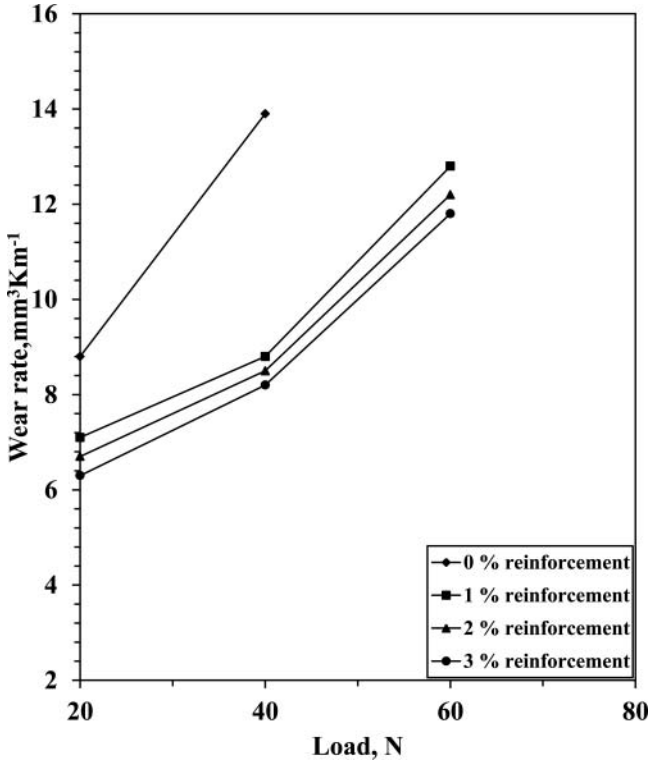

Fig. 5—Graph of wear rate vs. load at a speed of 2.618 m/s and test duration of 60 min.

of the materials. The transition in wear rate decreases with an increase in sliding velocity in all of the materials. The mild wear of the alloy is oxidation-dominated wear at low sliding velocity and low load. In the case of composites, due to the existence of silicon carbide and graphite particles, the oxide film is not continuous or dense. It is removed by friction forces in the sliding friction, resulting in oxidation-assisted mild abrasive wear. Hence, it can be considered that the dominant wear mechanism is the removal and reproduction of oxide film. Hence, this kind of wear is maintained until higher loads are employed under which condition the wear mechanism transforms from mild to severe wear. The morphology of the wear surface of the composite with 3% SiC and 3% graphite at loads from 20 to 80 N are respectively shown in Figs. 6a to 6d. The wear tracks in Figs. 6a and 6b show typical abrasive wear for the composite tested at low loads of 20 and 40 N, respectively. Hence, it can be said that the dominant wear mechanism is abrasive wear at low loads.

It was observed that at higher loads a transition occurs from mild to severe wear with a sharp rise in the wear rate due to higher applied loads, due to the increased friction and wear. In this condition, the removal and formation of oxide films is faster than that of mild oxidation and the wear mechanism changes to delamination wear for all of the composites, thereby resulting in a relatively increased wear rate.

Effect of Reinforcement on the Wear Rate

It follows from the observation that the reinforcement particles play a prominent role in enhanced wear resistance of the composites. It was found that the transition load increases with an increase in reinforcement content and the wear rate of the

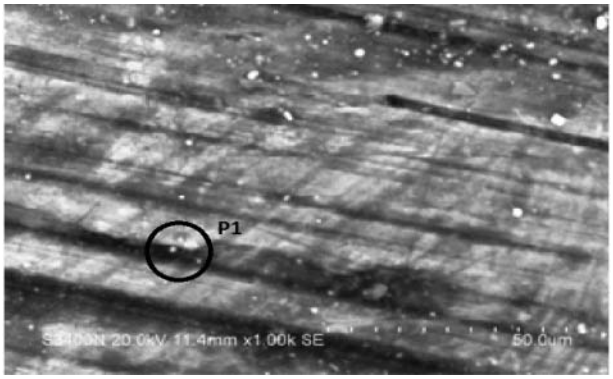

Fig. 6a—SEM showing the wear track morphology of 3% SiC and 3% graphite composites at 1.047 m/s and load of 20 N.

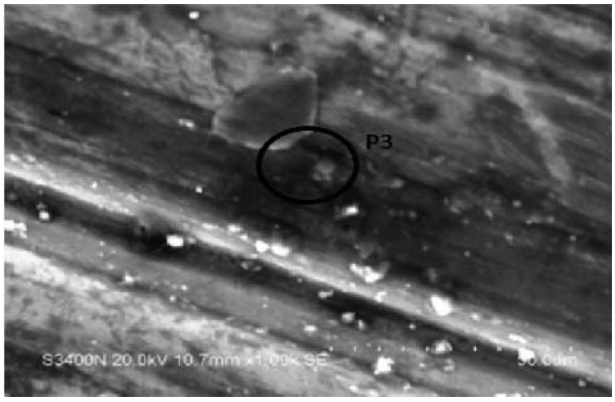

Fig. 6c—SEM showing wear track morphology of 3% Sic and 3% graphite composites at 1.047 m/s and load of 60 N.

composite was lower than that of the base alloy without silicon carbide and graphite reinforcements. This is obviously due to the release of SiC particles and graphite particles by the composite specimens to the mating surface during sliding, which provides resistance to wear. The removal of the reinforcement particles from the wear surface is clearly evident from the SEM micrograph in Fig. 6c. The black spots indicate places that were previously occupied by the reinforcement particles before being removed during the wear process. During the sliding contact wear, the SiC particles are sheared and the sheared layer adheres to the metal surfaces, aligning in the sliding direction, forming a thin film between mating surfaces. Moreover, the hard film of SiC has very limited ductility and has the ability to withstand stress without plastic deformation or fracture under low load conditions. It is well established that the wear rate and surface damage can be minimized if the plastic deformation of the material at the contact surface is prevented(Wang, et al. *(18)*; M.-J. Zhang, et al. *(19)*). Adhesion is observed to be slightly less severe for the composites than for the unreinforced alloy. It is a widely accepted fact that the wear rate of a material is inversely proportional to its hardness. Hardness tests were performed for the present case and the values are presented in Table 2. It follows from the results that the hardness of the base alloy was the lowest, whereas that of the specimen with 3% reinforcement was the highest. This increase in hardness values of the composites in comparison with the base alloy and also among themselves with increasing percentage of reinforcement can be attributed to the presence of hard particles of SiC. This, in fact, is the idea behind the addition of SiC particles along with graphite in the present case.

In studies on aluminum hybrid composites (Arrabal, et al. *(20)*; Altinkok, et al. *(21)*), the addition of SiC in both particulate and whisker form is reported to have lowered the wear rates, as well as shift the transition from delamination to adhesion at higher loads and sliding velocities. The presence of graphite reinforcement particles in the composites acts as a lubricant, which decreases the effect of abrasive wear. Demir, et al. *(22)*, in their study on hybrid composites, reported that the presence of ceramic material (Al_2O_3 particles) can increase the strength of the matrix and help sustain greater loads, whereas the presence of graphite delays the transition from mild wear to severe wear, which works effectively even at higher loads.

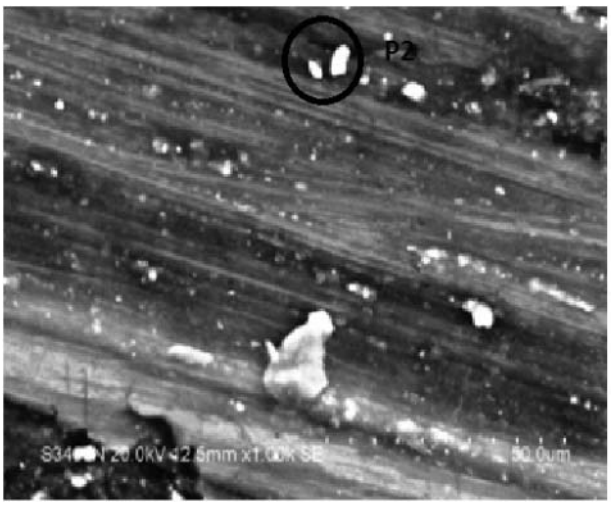

Fig. 6b—SEM showing wear track morphology of 3% SiC and 3% graphite composites at 1.047 m/s and load of 40 N.

Fig. 6d—SEM showing wear track morphology of 3% SiC and 3% graphite composites at 1.047 m/s and load of 80 N.

TABLE 2—HARDNESS VALUES OF THE SPECIMENS

Percentage of SiC and Graphite	Hardness (BHN)
0	61.1
1	62.8
2	64.3
3	66.2

SEM Analysis

Figures 7a to 7d show the SEM micrographs of the wear tracks of the specimens with 0, 1, 2, and 3% reinforcements, respectively, and Fig. 8 shows the SEM micrograph of the steel counterface on which the specimens slide. A brief comparison of the wear tracks of the specimens reveals that the base alloy experiences severe wear, whereas the one with 3% reinforcement shows the least wear.

The analysis of the wear track morphology of the specimens is also provided. However, for brevity and convenience, the analysis of only 3% SiC- and 3% graphite-reinforced composites at a sliding velocity of 1.047 m/s at various loads (20, 40, 60, and 80 N) is provided. Figures 6a to 6d show the SEM micrographs of the morphology study, and the analysis of EDS spectra for the marked is provided in Table 3. However, the explanation holds even for the composites with 1 and 2% reinforcement.

It follows from the SEM analysis that rough wear surfaces were produced on the surface of all specimens. The SEM micrograph of the worn surfaces shows areas that material has been removed from. As the load increases from low to higher values, the morphology of the worn surface gradually changes from fine scratches to distinct grooves, and damaged spots in the form of craters can be seen. At low loads of 20 and 40 N, the composite specimens show a mixed abrasion–plastic deformation mechanism as evident from Figs. 6a and 6b. Around the parallel grooves there is an obvious oxidative area and powder debris, which indicates abrasive and oxidization wear. This is because at the beginning of the dry sliding process, due to abrasive wear, the worn surface has slight grooves and debris. During sliding, the graphite smears on the worn surface and its lubricating effect decreases the influence of abrasive wear and hence the grooves become less intense. At the same time, the heat generated in the wear process due to friction at the interface is concentrated on the worn surface, causing it to oxidize easily. However, the test load is not high enough to peel off the oxidative alloys because they form continuous oxide area and, finally, oxidative alloys mixed with graphite form an oxide film. It was suggested that SiC particle reinforcement facilitates compaction of the

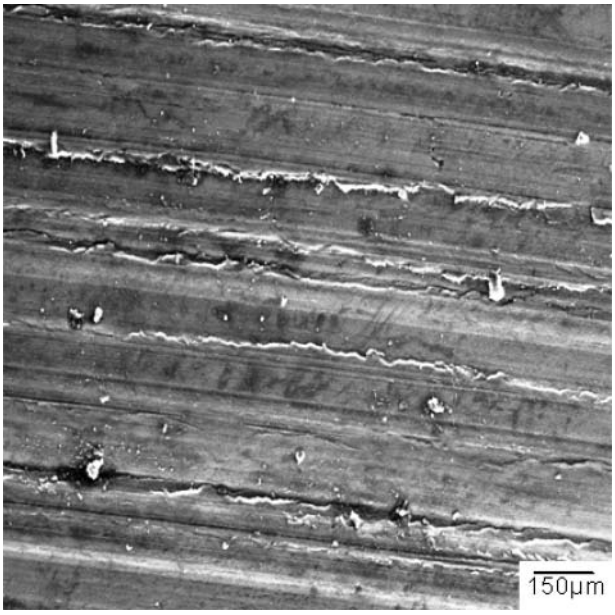

Fig. 7b—SEM micrograph of specimen with 1% reinforcement tested at a speed of 2.618 m/s and test duration of 60 min.

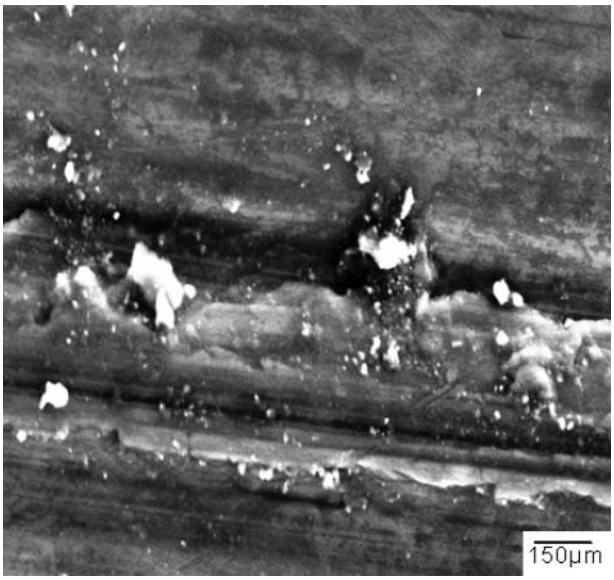

Fig. 7a—SEM micrograph of specimen with 0% reinforcement tested at a speed of 2.618 m/s and test duration of 60 min.

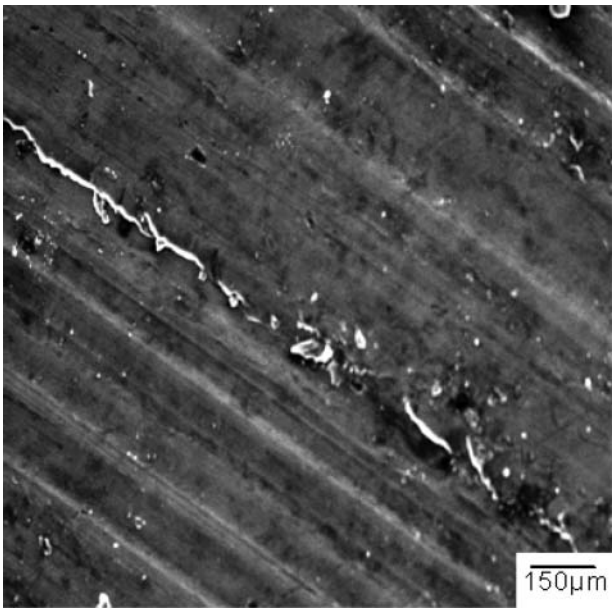

Fig. 7c—SEM micrograph of specimen with 2% reinforcement tested at a speed of 2.618 m/s and test duration of 60 min.

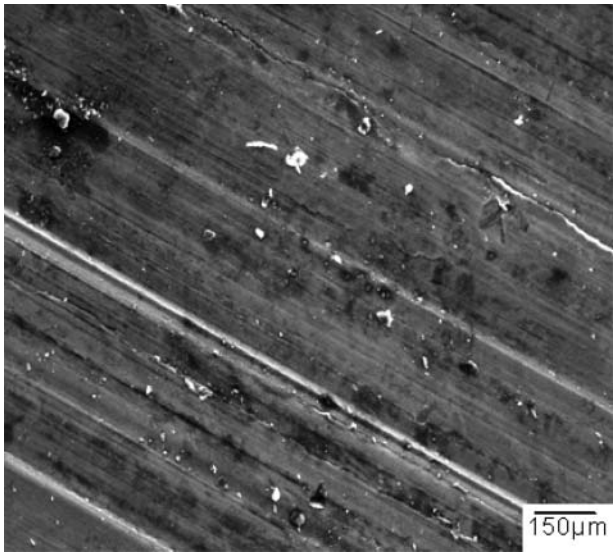

Fig. 7d—SEM micrograph of specimen with 3% reinforcement tested at a speed of 2.618 m/s and test duration of 60 min.

oxide film in between the particles (Kondoh, et al. *(23)*). The fragments of fractured SiC particles might also be mixed within the oxide layer, enhancing the hardness and wear resistance of the film (Kondoh, et al. *(23)*). Finally, the higher hardness of the composite provides better support for the oxide film, thus improving its stability and load-bearing capacity. The benefits of SiC particle reinforcement are evident in the generally lower wear rates of the composites when oxidation is present.

The alloy shows a transition at lower loads than the composites. It is observed that in the case of alloys, the rate of oxidation in metallic debris formed by severe wear of the unreinforced alloy is lower than the rate of generation of debris. This is because magnesium alloy is relatively ductile compared to composites and consequently it is more difficult to fracture. Because there are no hard reinforcing SiC particles to dig and gouge the metal out, there is less interaction between the pin and the counterface. This implies that heat due to friction will be lower than that of the composites and, as a result, the ambient temperature at the interface will obviously be lower. The lower temperature leads to a reduction in oxidation rates and hence reduces resistance to wear. On the other hand, the rate of oxidation of metallic debris produced by the pin or gouging of the counterface becomes faster than the rate of metallic debris formation. The composites have less ductility than the alloy, due to which they become fractured more easily and comminute to a size where

TABLE 3—MICROCHEMICAL ANALYSIS OF THE WORN SURFACES OF 3% SIC- AND 3% GRAPHITE-REINFORCED COMPOSITES

Points[a]	Elemental Composition (EDS Data) (wt%)						
P1 [6a]	C-4.7	O-6.7	Mg-77.8	Al-7.6	Si-2.1	Fe-0.6	Zn-0.5
P2 [6b]	C-5.1	O-7.3	Mg-75.9	Al-8.1	Si-2.2	Fe-0.8	Zn-0.6
P3 [6c]	C-5.3	O-6.3	Mg-76.1	Al-8.3	Si-2.5	Fe-1.1	Zn-0.4
P4 [6d]	C-5.5	O-6.1	Mg-75.3	Al-8.6	Si-2.8	Fe-1.2	Zn-0.5

[a]Numbers in brackets refer to the corresponding figure.

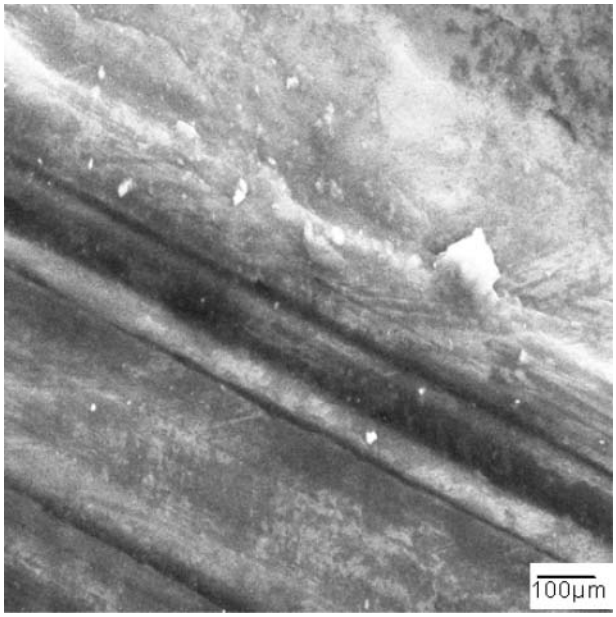

Fig. 8—SEM micrograph of the steel counterface.

spontaneous and complete oxidation occurs. In the case of composites, as the SiC particles dig in to the counterface and generate more friction, more heat will be produced during the process. The higher ambient temperature achieved by this process has the effect of significantly increasing the rate of oxidation of the metallic debris and hence contributes to the reduced wear rate or greater wear resistance than the unreinforced alloy.

The test load is high enough to peel off the oxidative alloys at 60 N, so it is difficult to form large continuous area of oxide film and the oxidative alloys take the form of powder debris or extrudes on the edge of grooves. This is shown in the SEM micrograph provided in Fig. 6c.

Examination of the wear debris reveals numerous flakes as observed in Fig. 9a. The composites with 3% reinforcement have larger strip debris and these large debris deteriorate the contact surface, whereas small debris influences the wear process

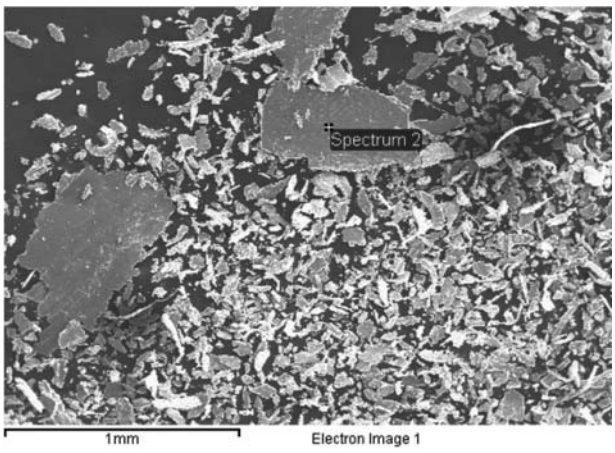

Fig. 9a—SEM morphology of wear debris of 3% SiC- and 3% graphite-reinforced composite tested at at 60 N load sliding velocity of 2.09 m/s.

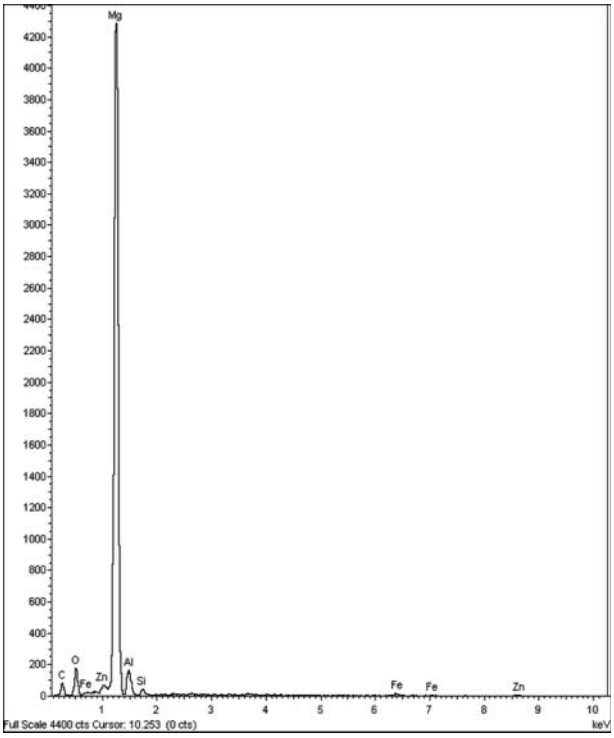

Fig. 9b—EDS spectra of wear debris of 3% SiC- and 3% graphite-reinforced composite tested at 60 N load and sliding velocity of 2.09 m/s.

to a lesser extent. Hence, large debris speeds up the transition from mild to severe wear. The EDS spectrum of corresponding debris is shown in Fig. 9b. In previous studies on Mg alloys and their composites, such features have been linked to the process of delamination (Kumar, et al. *(24)*; Lim, et al. *(25)*). This is a fatigue-related wear mechanism in which repeated sliding induces subsurface cracks that gradually grow and eventually shear to the surface, forming long, thin wear sheets (Findik *(26)*). Delamination is observed to be more extensive under the higher load of 60 N. Several investigators have reported the dominance of delamination in relation to load (Kondoh, et al. *(23)*; Kumar, et al. *(24)*; Lim, et al. *(25)*). Because delamination involves subsurface deformation, crack nucleation, and crack propagation (Rao and Das *(27)*), an increase in load will hasten these processes and produce greater wear. The pivotal role of crack formation and growth in delamination also accounts for the higher wear of the composites, as the SiCp–matrix interface provides additional void nucleation sites, as well as preferential crack propagation paths (Pathak, et al. *(28)*). In the present tests, wear rates for the composite are higher under the sliding conditions of 2.09 and 2.618 m/s under 60 and 80 N, respectively, where delamination is significant. This agrees with the findings of researchers (Jaykumar and Balamurugan *(29)*) who reported that alumina (Al_2O_3) particulate reinforcements in 6061 Al alloy were not beneficial when delamination was dominant. At higher speeds of up to 2 m/s, or under a lower load of 20 N, the presence of an oxide film protected the surfaces from delamination.

It can be concluded that at higher loads the main wear mechanism is delamination, causing excessive fracture of reinforcement and the matrix, resulting in deterioration of the wear resistance of the composite.

CONCLUSIONS

Pin-on-disc dry sliding wear tests were performed on AZ91 alloy and its composite specimens with various percentages of SiC and graphite reinforcement against a steel counterface under loads of 20 to 80 N and over a range of sliding velocities from 1.047 to 2.618 m/s. Three different wear mechanisms were found to operate under these conditions: abrasion, oxidation, and delamination. SiC and graphite particle–reinforced composites exhibited a lower wear rate than the unreinforced alloy specimens. The wear rate decreased with increasing hard reinforcement content as well as the graphite reinforcement in the composites. The wear rate of the composites as well as the base matrix alloy increased with an increase in applied load.

The dominant wear mechanism under a lower load of 20 N is abrasion and oxidation. The composites generally exhibit better wear resistance due to its superior load-bearing capacity and its ability to maintain a hard, stable, and continuous oxide film, which inhibits metal-to-metal contact with the steel counterface. A gradual transition from oxidation to abrasion and to delamination occurs with an increase in applied load. The wear resistance of the composites deteriorates as the presence of second phase promotes delamination wear. The wear rate increased above the critical load and at high sliding velocities. The transition to a high wear rate regime was induced by surface damage and material transfer to the counterface. The reinforcing SiC and graphite particles help in delaying the transition to the severe wear regime in the composites.

In view of their improved wear resistance, the SiC–graphite-reinforced magnesium alloy hybrid composites are possible candidate materials for wear resistance applications where lightweight alloys and composites are subjected to sliding motion, including automotive brakes, engine components, etc.

REFERENCES

(1) Aydin, M. and Findik, F. (2010), "Wear Properties of Magnesium Matrix Composites Reinforced with SiO_2 Particles," *Industrial Lubrication and Tribology*, **62**(4), pp 232–237.

(2) Qi, Q.-J., Liu, Y.-B., and Yang, X.-H. (2003), "Effects of Rare Earths on Friction and Wear Characteristics of Magnesium Alloy AZ91D," *Transactions of Nonferrous Metals Society of China*, **13**(1), pp 111–115.

(3) Zheng, R.-C., Wei, K., Xu, Y.-B., and Han, E.-H. (2001), "Recent Development and Application of Mg Alloys," *Acta Metallurgica Sinica*, **37** (7), pp 673–685.

(4) Zhai, W., Shi, X., Wang, M., Xu, Z., Yao, J., Song, S., and Zhang, Q. (2014), "Friction and Wear Properties of TiAl-Ti_3SiC_2-MoS_2 Composites Prepared by Spark Plasma Sintering," *Tribology Transactions*, **57** (3), pp 416–424.

(5) Zhang, H. J., Zhang, Z. Z., and Guo, F. (2011), "Studies of the Influence of Graphite and MoS_2 on the Tribological Behaviors of Hybrid PTFE/Nomex Fabric Composite," *Tribology Transactions*, **54**(3), pp 417–423.

(6) Zhang, L., Xiao, J., and Zhou, K. (2012), "Sliding Wear Behavior of Silver–Molybdenum Disulfide Composite," *Tribology Transactions*, **55**(4), pp 473–480.

(7) Rao, R. N., Das, S., Dixit, G., and Mondal, D. P. (2009), "Dry Sliding Wear Behaviour of Cast High Strength Aluminium Alloy (Al-Zn-Mg) and Hard Particle Composites," *Wear*, **267**(9/10), pp 1688–1695.

(8) Tu, J.-P. and Yang, Y.-S. (2000), "Tribological Behaviour of $Al_{18}B_4O_{33}$-Whisker-Reinforced Hypoeutectic Al-Si-Mg-Matrix Composites under Dry Sliding Conditions," *Composites Science and Technology*, **60**(9), pp 1801–1809.

(9) Lu, Y.-z., Qudong, W., Xiaoqin, Z., Wenjiang, D., Chunquan, Z., and Zhu, Y. (2000), "Effect of Rare Earths on the Microstructure, Properties and Fracture Behavior of Mg-Al Alloys," *Materials Science and Engineering A*, **278**(1/2), pp 66–76.

(10) Gu, J.-H., Zhang, X.-N., and Gu, M.-Y. (2004), "Mechanical Properties and Damping Capacity of (SiCp+Al2O3·SiO2f)/Mg Hybrid Metal Matrix Composites," *Journal of Alloys and Compounds*, **385**(13), pp 104–108.

(11) Qi, Q.-J., Liu, Y.-B., and Yang, X.-H. (2003), "Friction and Wear Characteristics of Mg-Al Alloy Containing Rare Earths," *Journal of Rare Earths*, **21**(2), pp157–162.

(12) Baradeswaran, A. and Elaya Perumal, A. (2014), "Study on Mechanical and Wear Properties of Al 7075/Al_2O_3/Graphite Hybrid Composites," *Composites B*, **56**, pp 464–471.

(13) Ram Prabhu, T., Varma, V. K., and Srikanth, V. (2014), "Tribological and Mechanical Behavior of Multilayer Cu/SiC + Gr Hybrid Composites for Brake Friction Material Applications," *Wear*, **317**, pp 201–212.

(14) Zhan, Y. and Zhang, G. (2006), "The Role of Graphite Particles in the High Temperature Wear of Copper Hybrid Composites against Steel," *Materials & Design*, **27**, pp 79–84.

(15) Sahin, Y. and Acilar, M. (2003), "Production and Properties of SiCp-Reinforced Aluminium Alloy Composites," *Composites A*, **34**(8), pp 709–718.

(16) Sharma, S. C., Anand, B., and Krishna, M. (2000), "Evaluation of Sliding Wear Behaviour of Feldspar Particle–Reinforced Magnesium Alloy Composites," *Wear*, **241**, pp 33–40.

(17) Mondal, A. K. and Kumar, S. (2009), "Dry Sliding Wear Behaviour of Magnesium Alloy Based Hybrid Composites in the Longitudinal Direction," *Wear*, **267**, pp 458–466.

(18) Wang, H. Y., Jiang, Q.C., Zhao, Y.Q., Zhao, F., Ma, B.X., and Wang, Y. (2004), "Fabrication of TiB_2 and TiB_2-TiC Particulates Reinforced Magnesium Matrix Composites," *Materials Science and Engineering A*, **372** (1/2), pp 109–114.

(19) Zhang, M.-J., Yong-Bing, L., Xiao-Hong, Y., Jian, A., and Ke-Shuai, L. (2004), "Effect of Graphite Particle Size on Wear Property of Graphite and Al_2O_3 Reinforced AZ91D-0.8%Ce Composites," *Transactions of Nonferrous Metals Society of China*, **18** (1), pp 273–277.

(20) Arrabal, R., Pardo, A., Merino, M.C., Mohedano, M., Casajus, P., Paucer, K., Matykina, E. (2011), "Oxidation Behavior of AZ91D Magnesium Alloy Containing Nd or Gd," *Oxidation of Metals*, **76**, pp 433–450.

(21) Altinkok, N., Ozsert, I., and Findik, F. (2013), "Dry Sliding Wear Behavior of Al_2O_3/SiC Particles Reinforced Aluminum Based MMCs Fabricated by Stir Casting Methods," *Acta Physica Polonica*, **124**(1), pp 11–19.

(22) Demir, A., Altinkok, N., and Findik, F. (2004), "The Wear Behavior of Dual Ceramic Particles (Al_2O_3/SiC) Reinforced Al Matrix Composites," *Key Engineering Materials*, **264–268**, pp 1079–1082.

(23) Kondoh, K., Tsuzuki, R., and Yuasa, E. (2005), "Tribological Properties of Magnesium Matrix Composite Alloys Dispersed with Mg_2Si Particles," *Advances in Technology of Materials and Materials Processing Journal*, **7**(1), pp 33–36.

(24) Kumar, B. V. M., Basu, B., Murthy, V. S. R., and Gupta, M. (2005), "The Role of Tribochemistry on Fretting Wear of Mg-SiC Particulate Composites," *Composites A*, **36**, pp 13–23.

(25) Lim, C. Y. H., Lim, S. C., and Gupta, M. (2003), "Wear Behavior of SiCp-Reinforced Magnesium Matrix Composites," *Wear*, **255**, pp 629–637.

(26) Findik, F. (2014), "Latest Progress on Tribological Properties of Industrial Materials," *Materials & Design*, **57**, pp 218–244.

(27) Rao, R. N. and Das, S. (2010), "Effect of Matrix Alloy and Influence of SiC Particles on the Sliding Wear Behavior of Aluminum Alloy Composites," *Materials & Design*, **31**, pp 1200–1207.

(28) Pathak, J. P., Singh, J. K., and Mohan, S. (2006), "Synthesis and Characterization of Aluminium–Silicon Carbide Composites," *Indian Journal of Engineering and Materials Science*, **13**, pp 238–246.

(29) Jaykumar, L. and Balamurugan, K. (2014), "Reciprocating Wear Behavior of 7075 Al/Al_2O_3 Composites," *International Journal of Refractory Metals and Hard Materials*, **46**, pp 137–144.